Sensitivity Analysis of PCDR35 Radar

Lubos Rejfek [1], Ondrej Fiser [1], David Matousek [1], Ladislav Beran [1], Pavel Chmelar [1]
[1] University of Pardubice Faculty of Electrical Engineering and Informatics Department of Electrical Engineering, Pardubice Studentská 95, Czech Republic
E-mail: Lubos.Rejfek@upce.cz

***Abstract* - This conference paper is aimed at the analysis of the frequency modulated interrupted continuous wave radar (PCDR35). This radar was developed under the Institute of Atmospheric Physic Czech Academy of Sciences leadership. A primary aim of this radar is the monitoring of meteorological targets (rain cells, hail stones and other). In this paper a radar measurement of the corner reflector with the theoretical reflectivity determination are compared. In the last part of this paper an evaluation of this radar and possible modifications (classical FMCW) are described.**

Keywords* - *FMICW radar; spectral analyse; meteorological targets; radar sensitivity; radar validation

I. INTRODUCTION

Our FMICW (Frequency Modulated Interrupted Continuous Wave) radar is composed from three parts. The first radar part is a frequency base. This part makes a frequency sweeping. The second part is a transmitter. This part transforms frequencies of the signals to the transmitted frequency and amplifies the signal. The last part is a receiver. Principal scheme of the radar is in Fig. 1.

The FMICW radar timing diagram is shown in Fig. 2, parameters of our radar are described in [1]. From this graph you can see that output from the radar is a difference between two frequencies (transmitted and received). Signals from the FMICW radars are primary processed by the spectral analysis. Parametric or non-parametric methods are used for the signals' spectral analysis. Non-parametric method is for example Fourier transform. Parametric methods are based on two principles. The first group is based on auto covariance matrix decomposition (MUSIC, Eigen Value Algorithm, Pisarenko, Minimum Norm. algorithm) and the second group is based on the digital filters (AR (auto regressive) model, MA (moving average) model, ARMA model). Power spectral density (PSD) methods are described for example in [2, 3, 4, 5 and 6]. An example of the frequency analysis is shown in Fig. 3. Spectral analysis can be made in two dimensions. It is described in [7].

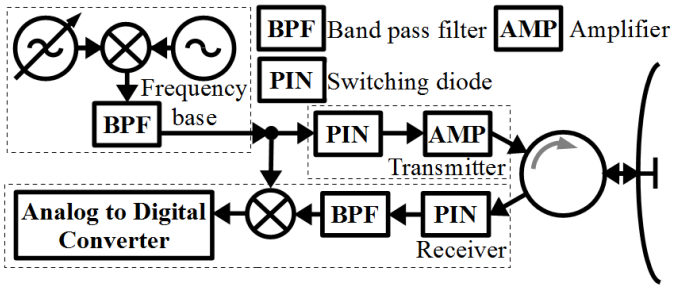

Figure 1. Principial scheme of the FMICW radar. [1]

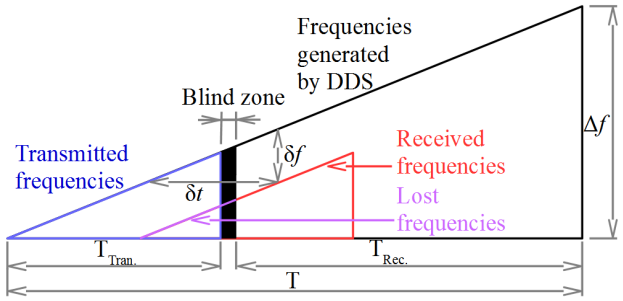

Figure 2. Timing diagram of FMICW radar. [1]

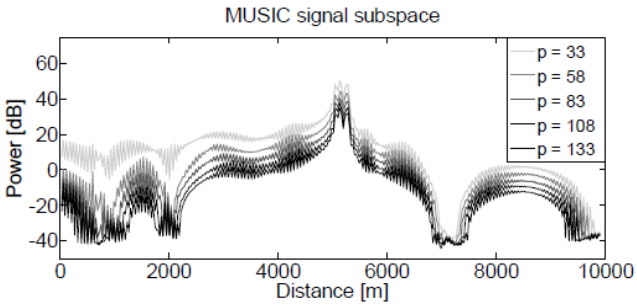

Figure 3. Example of the spectral analysis of the signal from the FMICW radar by the multi signal clasification (MUSIC) method. [2]

Spectral analyses are used for the primary FMICW radar signal processing. A problem of the FMICW radars is lost part of a reflected signal. This makes changes in the power and the real reflected area is estimated wrongly. This complication is described in [3].

II. CHARACTERISTICS OF THE CONSIDERED TARGETS

Our intention is the using of PCDR35 radar for the meteorological targets monitoring. The reflected power can be calculated according the equation (1). The transmitted power is 37 dBm, the antenna gain is 45 dBi. We will use this radar for the ranges up to 10 km. Some improvements for the meteorological targets adaptation were realized in this radar. The most important improving is the cancelation of the noise transmitted from the output amplifier to the receiver.

$$P_r = \frac{P_t \cdot G_t}{4 \cdot \pi \cdot R^2} \cdot \sigma \cdot \frac{1}{4 \cdot \pi \cdot R^2} \cdot A_{eff}\,, \qquad (1)$$

presented in [8], where P_t is transmitted power, P_r is received power, R is range, σ is reflective area, A_{eff} is the effective area of the radar receiving antenna.

The radar reflectivity η is directly measured by radar and it is defined by the equation (2)

$$\eta = \frac{\sum \sigma(D)}{V} = \frac{\sum \sigma(D)}{S \cdot h} = \frac{\sum \sigma(D)}{\frac{\pi \cdot \Theta^2 \cdot R^2 \cdot c_0 \cdot \tau}{8}} \qquad (2)$$

where σ is the back scattering cross section (BSCS) of a cloud particle (SUM symbol in (1) represent the sum of BSCS of all particles in the radar volume V (pixel), θ is the 3 dB beam width (in radians) and R is the distance of the target, c_0 is the light speed and τ is the pulse length.

The received power P_r is given by the simplified radar equation (3). The radar reflectivity η is dependent on a radar frequency. In order to eliminate this, the equivalent radar reflectivity factor z_e [$mm^6\ m^{-3}$] (small letter z) is used which is defined as (4), the back scattering cross section of the droplet of diameter D is approximatively given by (5) and fraction in this formula represents the frequency dependence in Rayleigh region supposing it is similar also out of Rayleigh region, i.e. also for $D > 0{,}3\ \lambda$), both λ and D must be in [mm]. Auxiliary variable $\boldsymbol{K}$ is given by next expression (6). Principle is in Fig.4.

$$P_r = C_r \frac{\eta}{R^2} \qquad (3)$$

$$z_e = \frac{\lambda^4}{\pi^5 |\mathrm{K}|^2}\ \eta \qquad (4)$$

$$\sigma = \frac{\pi^5 |K|^2}{\lambda^4}\ D^6 \qquad (5)$$

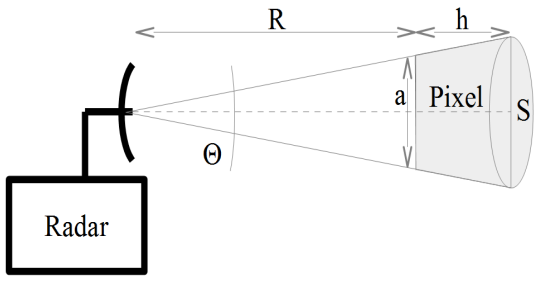

Figure 4. Principle of signal propagation, it is more described in [9].

$$K = \frac{m^2 - 1}{m^2 + 2} = \frac{\varepsilon_r - 1}{\varepsilon_r + 2}, \qquad (6)$$

where C_r is the radar constant depending on radar parameters and R is the target distance, the wavelength λ must be in [mm]. This is because, in special case of so called Rayleigh region ($D < 0.3\ \lambda$), $\boldsymbol{m}$ ($\boldsymbol{\varepsilon_r}$) is the complex refractivity index of the cloud droplet (relative permittivity), both quantities are frequency dependent. The refractivity index of water for 35 GHz is 4.9 + i 2.8, the corresponding complex relative permittivity is $\varepsilon_r = 16 + i\ 27$, $\boldsymbol{K^2}$ is approx. 0.91 for 35 GHz.

In a practice, the radar reflectivity factor $\mathbf{Z}_e$ (capital letter Z) is often given in dBZ after

$$Z_e = 10 \cdot \log_{10}(z_e) \qquad (7)$$

In the case of cloud droplets, the Z_e value is from -32 to -15 dBZ. Combining (7) and (4) one can obtain equation (8).

$$\eta = \frac{\pi^5 \cdot |K|^2}{\lambda^4} \cdot 10^{\frac{Z_e}{10}} \qquad (8)$$

and again, wavelength λ must be in [mm]. From previous expressions we can derive an expression for the equivalent back scattering cross section A_{eff}, which simulates an equivalent point target corresponding to a cloud of the radar reflectivity factor Z_e (in dBZ) at R distance:

$$A_{eff} = k \cdot V \cdot \eta = k \cdot \frac{\pi \cdot \Theta^2 \cdot R^2}{4} \cdot h \cdot \frac{\pi^{5\cdot} \cdot |K|}{\lambda^4} \cdot 10^{\frac{Z_e}{10}}, \qquad (9)$$

where the pixel length h is part of equation (2), λ is in [mm] again, k is correction factor. The target distance is determined by our radar by (12), i.e.

The power correction factor k is equal to 1 if a signal is coming to the receiver all time it is open, i.e. 66 us. In other cases, it is

$$k = \frac{s}{2 \cdot f_s \cdot 66}, \qquad (10)$$

where s/f_s must be in microseconds.

III. Measurements in the Terrain

The radar system was tested in the terrain during summer 2016. The radar placement is shown in Fig. 5. The radar aiming is realized by a radio beacon. A radio beacon was composed from a battery source (blue arrow), a generator (red arrow) and an antenna (yellow arrow). This station is shown in Fig. 6. In the first step a transmitter in the radar was disconnected and a radio beacon was placed on a defined position. After aiming (it is shown in Fig. 7 – red arrow), the radio beacon was removed. On his position the corner reflector was placed and the radar transmitter was switched on. Fig. 8 shows the station positions for the measurement. The red arrow is for the corner

reflector, a point in the village is the radar station and the green arrow is a forest in the background. The distance between the corner reflector and the radar is approx. 570 meters and the distance between the radar and a forest is approx. 780 meters. The used corner reflector has edge length 320 mm. The reflective area for the frequency 35.4 GHz is according to equation (11) 611 m^2.

The signal reflected from a corner reflector is shown in Fig. 9. The first marked point is the last part of the signal reflected from a corner reflector (A), the second marked point is the last part reflected from a forest in the background (B) and the last marked point is maximal value of the noise level (C). From this graph, we can estimate that target is (according to (12)) in the distance 585 meters and the resolution between two points is 15 meters. The distance of the forest is, according to this equation 795 meters. We can see that in time dimension signal noise ratio (SNR) for one realization is approx. 32 dB for the used the corner reflector as a target.

$$S_{E\max} = \frac{4 \cdot \pi}{3} \cdot \frac{a^4}{\lambda^2} \text{ [8]} \qquad (11)$$

Figure 5. FMICW radar PCDR35.

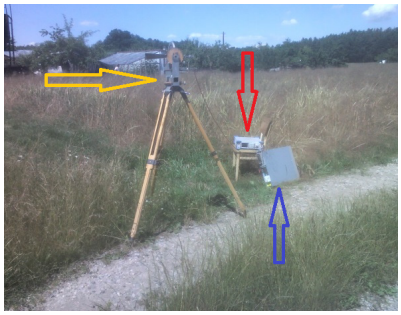

Figure 6. Radio beacon for navigation of the radar.

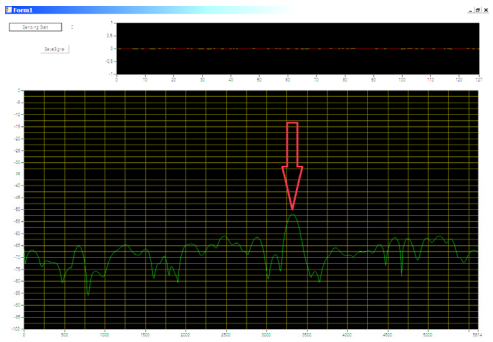

Figure 7. Detection of the radio beacon.

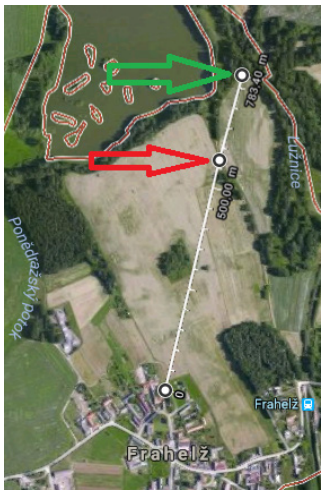

Figure 8. Position of the stations during the measurements.

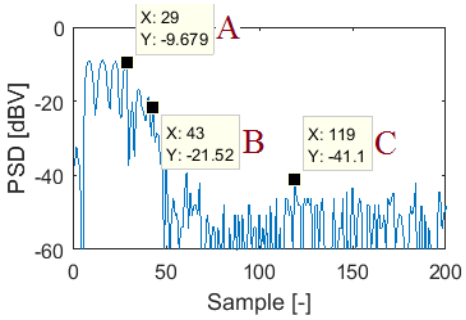

Figure 9. Example of the reflected signal (clutter and reference target – corner reflector).

$$R = \frac{c_0 \cdot s}{2 \cdot f_s} + \frac{c_0 \cdot t_{BZ}}{2}, \qquad (12)$$

where c_0 is the speed of light, f_s is the sampling frequency, s is a sample and t_{BZ} is the time for the blind zone.

The measured data processing by the 2D FFT algorithm is shown in Fig. 10 and 11. The first figure shows only a clutter, the second figure shows a clutter and a corner reflector. In this case SNR is approx. 55 dB. The minimal detectable reflective area for the radar PCDR35 in the distance 580 meters was derived from the equation (13), this area is 0.0199 m^2.

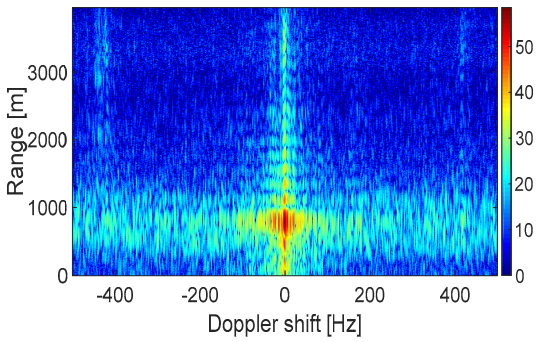

Figure 10. Clutter withouth corner reflector measured by the PCDR35 radar (forest in distance approx. 780 m).

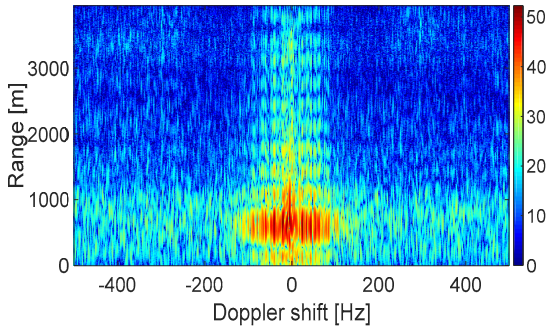

Figure 11. Corner reflector with clutter measured by the PCDR35 radar.

$$10 \cdot \log_{10} \sigma_{\min} = 10 \cdot \log_{10} \sigma - (SNR - SNR_{\min}), \quad (13)$$

where σ is the reflective area of the corner reflector (611 m^2), *SNR* is the signal noise ratio in the received signal and SNR_{min} is a minimal signal noise ratio (10 dB).

IV. Comparison of the Results with Theory

Reflective areas of few meteorological targets types for different distances are shown in Fig. 12. Blue curves are for the rain cells and gray curves are for the clouds. These curves were obtained by an equations' utilization from the capture 2. Green curves are minimal detectable reflective areas (light green for one signal and dark green for the coherent integration). These curves were obtained from the equations' combination from captures 1 (dependence on the range) and 3 (measured SNR) (minimal detectable area in known distance was transform to function of the distance) and powers are modified in accordance with knowledges from [3] (estimated power is depended on the target distance). Modification of the power is represented by the curve in Fig. 13. The equation for this curve is (14). These green curves are borderlines. Targets with bigger reflective area (σ) in tested distance are detectable.

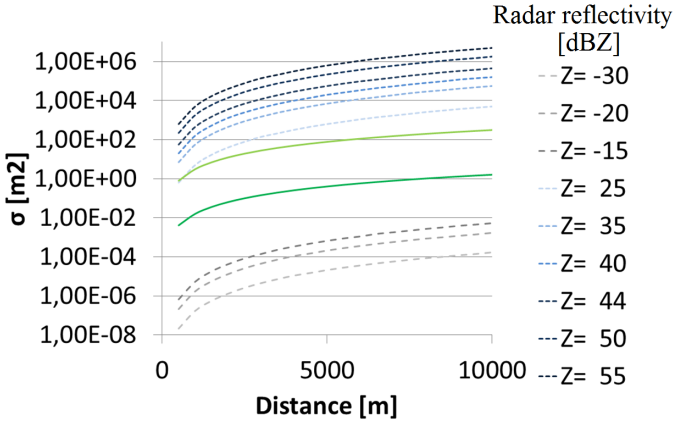

Figure 12. Comparison of the reflective areas with minimal detectable areas.

$$Coefficient = \frac{x^2}{400} + \frac{x}{151.51} - 0.2513, \quad (14)$$

where x is the number of samples with a reflected signal.

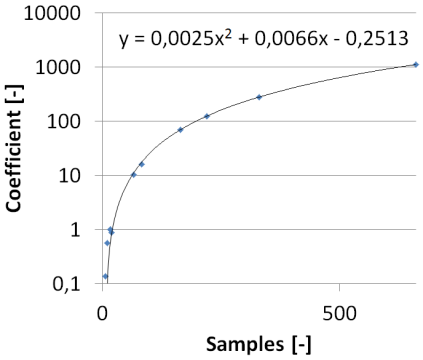

Figure 13. Modification of the power in dependence of the signal length.

V. Conclusion

The real radar PCDR35 measurement results were compared with the theory concerning meteorological targets in this paper. From Fig. 12 it is possible to conclude that after last radar PCDR35 modifications, the radar can be used for rain cells monitoring, but this radar cannot be used for the cloud detection with this configuration.

A possible modification to extending radar sensitivity is the change of the principle from FMICW to the classical FMCW radar, but this is an expensive alternation, which cannot be realized in present.

VI. Acknowledgement

The research was supported by the Internal Grant Agency of University of Pardubice, the project No. SGS_2017_030.

VII. References

[1] L. Rejfek, Z. Mosna, J. Urbar, and P. K. Knizova, "System for Automatic Detection and Analysis of Targets in FMICW Radar Signal," Journal of Electrical Engineering, 67(1), pp. 36-41.

[2] L. Rejfek, D. Buresova, O. Fiser and V. Brazda, "Comparison of parametric methods for radar signal processing," Proceedings of 25th International Conference Radioelektronika, RADIOELEKTRONIKA 2015 2015, pp. 141-144.

[3] L. Rejfek, L. Beran, and O. Fiser, "Correction of radar received signal," Proceedings of 25th International Conference Radioelektronika, RADIOELEKTRONIKA 2015 2015, pp. 191-194.

[4] Z. Smekal, "Číslicové zpracování signálů," Vysoké Učení Technické v Brně, Fakulta elektrotechniky a komunikačních technologií, 2009, skriptum, p. 208

[5] D. Mandic, "Spectral Estimation and Adaptive Signal Processing," Imperial College London, Department of Electrical and Electronic Engineering, 2012. Lectures.

[6] P. Stoica, and R. Moses, "Introduction to Spectral Analysis," Upper Saddle River, NJ: Prentice Hall, 1997.

[7] M. Mandlik, and V. Brazda, "FMICW radar simulator," Proceedings of 25th International Conference Radioelektronika, RADIOELEKTRONIKA 2015 2015, pp. 317-320.

[8] J. Stastny, S. Cheung, G. Wiafe, K. Agyekum, and H. Greidanus, "Application of RADAR Corner Reflectors for the Detection of Small Vessels in Synthetic Aperture Radar." IEEE Journal of Selected Topics in Applied Earth Observations and Remote Sensing, 2014

[9] L. Rejfek, P. Bezousek, O. Fiser, and V. Bazda, "FMICW radar simulator at the frequency 35.4 GHz," 2014 24th International Conference Radioelektronika, RADIOELEKTRONIKA 2014 Proceedings 2014.